Plant Growth Regul (2008) 54:165–177
DOI 10.1007/s10725-007-9239-2

ORIGINAL PAPER

Characteristics of adventitious root formation in cotyledon segments of mango (*Mangifera indica* L. cv. Zihua): two induction patterns, histological origins and the relationship with polar auxin transport

Yun-He Li · Qi-Zhu Chen · Jie-Ning Xiao · Yun-Feng Chen · Xiao-Ju Li · Christian Staehelin · Xue-Lin Huang

Received: 8 May 2007 / Accepted: 19 November 2007 / Published online: 5 December 2007

Abstract Cotyledon segments derived from zygote embryos of mango (*Mangifera indica* L. cv. Zihua) were cultured on agar medium for 28 days. Depending on different pre-treatments with plant growth regulators, two distinct patterns of adventitious roots were observed. A first pattern of adventitious roots was seen at the proximal cut surface, whereas no roots were formed on the opposite, distal cut surface. The rooting ability depended on the segment length and was significantly promoted by pre-treatment of embryos with indol-3-acetic acid (IAA) or indole-3-butyric acid (IBA) for 1 h. A pre-treatment with the auxin transport inhibitor 2,3,5-triiodobenzoic acid (TIBA) completely inhibited adventitious root formation on proximal cut surfaces. A second pattern of roots was observed on abaxial surfaces of cotyledon segments when embryos were pre-treated with 2,700 μM 1-naphthalenacetic acid (NAA) for 1 h. Histological observations indicated that both patterns of adventitious roots originated from parenchymal cells, but developmental directions of the root primordia were different. A polar auxin transport assay was used to demonstrate transport of [^{3}H] indole-3-acetic acid (IAA) in cotyledon segments from the distal to the proximal cut surface. In conclusion, we suggest that polar auxin transport plays a role in adventitious root formation at the proximal cut surface, whereas NAA levels (influx by diffusion; carrier mediated efflux) seem to control development of adventitious roots on the abaxial surface of cotyledon segments.

Keywords Adventitious root · Cotyledon segment · *Mangifera indica* L. · 1-Naphthalenacetic acid (NAA) · Polar auxin transport (PAT) · Vascular tissue

Abbreviations

AM	Agar medium (0.7%, w/v) without plant growth regulators and sucrose
2,4-D	2,4-Dichlorophenoxyacetic acid
DCS	Distal cut surface
FAA	Formalin:acetic acid:ethanol (5:5:90 v/v/v)
IAA	Indole-3-acetic acid
IBA	Indole-3-butyric acid
LCS	Longitudinal cut surface
NAA	1-Naphthalenacetic acid
PAT	Polar auxin transport

Y.-H. Li · Q.-Z. Chen · J.-N. Xiao · Y.-F. Chen · X.-J. Li · X.-L. Huang (✉)
The Key Laboratory of Gene Engineering of the Ministry of Education, School of Life Sciences, Sun Yat-sen (Zhongshan) University, 135, Xin Gang West Road, Guangzhou 510275, China
e-mail: huangxl@mail.sysu.edu.cn

J.-N. Xiao
Department of Biology, Guangzhou University, Guangzhou 510400, China

C. Staehelin
State Key Laboratory of Biocontrol, School of Life Sciences, Sun Yat-sen (Zhongshan) University, Guangzhou 510275, China

PCS Proximal cut surface
TIBA 2,3,5-Triiodobenzoic acid

Introduction

Adventitious root formation is an important step in plant vegetative propagation and mainly controlled by genetic, physiological, physical and chemical factors (De Klerk et al. 1999). The effects of plant hormones and other factors on rooting have been extensively examined in various plant species (Blakesley 1994; De Klerk et al. 1999; Jarvis and Shaheed 1986; Kevers et al. 1997; Steffens et al. 2006). Auxin is the primary signal for adventitious root formation (Blakesley 1994), and endogenous auxin, indole-3-acetic acid (IAA), plays a key role in adventitious rooting (De Klerk et al. 1999). IAA is locally synthesized in the plant's growing regions such as shoot apex, young leaves and developing seeds (Ljung et al. 2001; Normanly et al. 1993). In general, IAA is basipetally transported from the shoot apex to the roots by a process termed polar auxin transport (PAT). The importance of PAT in adventitious rooting of hypocotyl cuttings has been reported in various studies (e.g., Liu and Reid 1992; López Nicolás et al. 2004).

Cotyledon segments derived from zygote embryos are suitable tissues for studying adventitious root formation. In these systems, roots can be easily induced in the absence of exogenous plant growth regulators (Ermel et al. 2000; Gutmann et al. 1996; Jay-Allemand et al. 1991). In walnut cotyledons for example, the mechanisms of adventitious root formation are different from those of primary or lateral root formation (Ermel et al. 2000). To our knowledge, except for certain effects of ethylene on adventitious rooting of cotyledon segments (Gonzalez et al. 1991; Mensuali-Sodi et al. 1995), there is still little information about the role of plant growth regulators in adventitious root formation of cotyledon segment from tree species; moreover, the role of PAT in adventitious root formation of cotyledon segment from tree species has not been investigated so far.

In this study, we report that mango (*Mangifera indica* L. cv. Zihua) cotyledon segments show two distinct patterns of adventitious roots. Root development was observed at the proximal cut surface (PCS) of cotyledon segments, whereas no roots emerged on the opposite, distal cut surface (DCS). A pretreatment of embryos with high concentrations of NAA resulted in another pattern of adventitious roots, which emerged on abaxial surfaces of cotyledon segments. In order to study the role of PAT in adventitious root formation, we performed labeling experiments with [^{3}H]IAA and compared the effects of IAA, IBA, 2,4-dichlorophenoxyacetic acid (2,4-D), NAA and the PAT inhibitor TIBA on the rooting ability of cotyledon segments.

Materials and methods

Induction of adventitious roots in cotyledon segments

Mature mango (*Mangifera indica* L. cv. Zihua) fruits were collected at the Guangzhou Fruit Research Institute (Guangzhou, China). Embryos of similar size and fresh weight were selected after they have been dissected from mango fruits. Embryos were rinsed with tap water for 1 h and then surface-sterilized with 10% (v/v) commercial bleach for 10 min. After five washes in sterile distilled water, embryos were placed on sterile filter paper and cotyledons were cut into segments (the embryo axis was also excised and discarded). The length of segments depended on the purpose of the experiment. All cotyledon segments used in this study had a minimal distance of 1 cm from the embryo axis (Fig. 1b).

For induction of adventitious roots, two segments were horizontally placed in a 150 ml Erlenmeyer flask that contained 20 ml of 0.7% (w/v) AM (autoclaved agar medium without plant growth regulators and sucrose; pH adjusted to 5.8). In this system, abaxial surfaces of cotyledon segments had a direct contact with the AM. The explants were cultured at 28 ± 2°C in the dark for the indicated period.

To evaluate the effects of cut directions on root formation, cotyledons were crossly (Fig. 1b) or longitudinally (Fig. 1c) cut into 2-cm segments. Unless indicated otherwise, all cotyledon segments were crossly cut, because preliminary studies showed that no roots emerged from longitudinal cut surfaces (LCS).

In order to compare the effects of segment length on rooting ability, the selected cotyledons were crossly cut into lengths of 0.2, 0.5, 1 and 2 cm, respectively. Cotyledon segments were cultured on AM at 28 ± 2°C

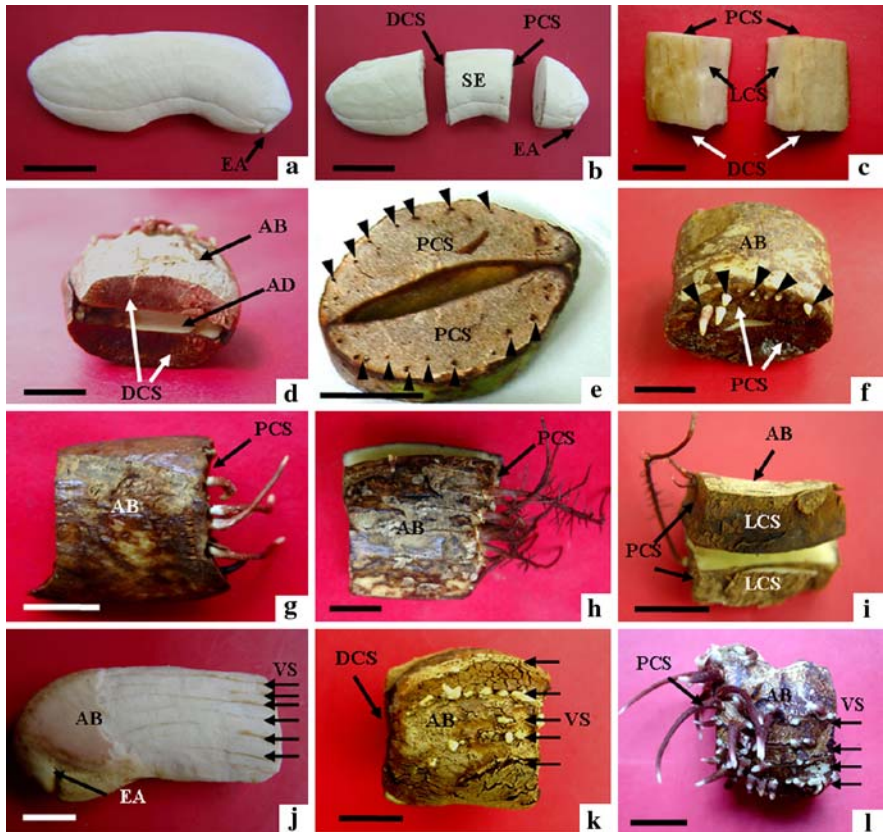

Fig. 1 Patterns of adventitious root formation in mango (*Mangifera indica* L. cv. Zihua) cotyledon segments. The pattern of adventitious roots depended on the pre-treatment with NAA. Mango embryos were first pre-treated with 2,700 μM NAA for 1 h (**k–l**) or not (**c–i**). After removal of the embryo axis (EA) (**a**), mango cotyledons were cut crossly (**b**) or longitudinally (**c**) into 2 cm long segments, which were cultured on AM for the indicated days. (**c–i**) A first pattern of adventitious root formation at the PCS; (**j–l**) A second pattern of adventitious root formation induced by a pre-treatment with 2,700 μM NAA. (**a**) Mature embryo, about 6 cm long. (**b**) An about 2-cm long cotyledon segment (SE) was crossly excised at a distance of 1 cm from the embryo axis (EA). The cut surface close to the embryo axis was defined as proximal cut surface (PCS), and the opposite surface as distal cut surface (DCS). (**c**) The 2-cm long cross segment (SE) in (**b**) was longitudinally cut into two equal 2-cm longitudinal segments, resulting in longitudinal cut surfaces (LCS). (**d**) The DCS of a cotyledon segment with abaxial (AB) and adaxial (AD) surfaces. (**e**) The PCS of a cotyledon segment cultured for 3 days. Vascular bundles (*arrowheads*) are located in the peripheral region of the PCS. (**f**) A first pattern of adventitious roots (*arrowheads*) was observed on the PCS after segments were cultured for 15 days on AM. (**g**) The same pattern of adventitious roots on the PCS (day 21). No roots emerged on the DCS. (**h**) The same pattern of adventitious roots (day 28). Roots were only formed on PCS but not on DCS and abaxial surfaces. (**i**) For longitudinal segments, adventitious roots emerged on the PCS, but not on DCS, LCS or abaxial surfaces (day 28). (**j**) The direction of vascular strands (VS) in a cotyledon (indicated by *arrowheads*) was almost parallel to the long axis of the cotyledon. (**k**) A different pattern of adventitious roots was observed on abaxial surfaces of cotyledon segments, which were pre-treated with 2,700 μM NAA (day 10). (**l**) A cotyledon segment pre-treated with 2,700 μM NAA (day 14). In addition to adventitious root formation on the PCS, adventitious roots are visible on the abaxial surface. Roots on abaxial surfaces emerged along several narrow 'canal' regions, where vascular strands are located. Bars in (**a**), (**b**) = 2 cm, bars in (**c–l**) = 1 cm. Abbreviations: AB, abaxial surface; AD, adaxial surface; DCS, distal cut surface; EA, embryo axis; LCS, longitudinal cut surface; PCS, proximal cut surface; SE, cross segment; VS, vascular strands

in the dark (Table 1). At the time of harvest (after 28 days incubation if not otherwise mentioned), the percentage of rooting, the number of adventitious roots and the rooting time were recorded for roots longer than 2 mm. Percentage of rooting = (number of rooted segments/number of tested segments) × 100%. Number of adventitious roots = sum of the roots of rooted segments/number of rooted segments. Rooting time =

Table 1 Effect of cotyledon segment length on formation of adventitious roots on the PCS

Length (cm)	Percentage of rooting (%)	Rooting time (days)	Number of adventitious roots per segment
2	77.5 ± 4.8a	13.2 ± 0.5b	6.9 ± 0.5a
1	70.0 ± 5.8a	13.7 ± 0.6ab	4.0 ± 0.4b
0.5	27.5 ± 4.1b	15.2 ± 0.6a	1.7 ± 0.3c
0.2	0	–	0

Values represent means ± SE from three independent experiments with 30 segments per treatment. Values within a column followed by the same letter are not significantly ($P > 0.05$) different according to Duncan's multiple range test

sum of the days required for first root emergence of rooted segments/number of rooted segments.

Chemicals and radiochemical

[^{3}H]IAA (3-[5(n)-^{3}H] indolylacetic acid, specific activity 851 GBq mmol^{-1} or 23 Ci mmol^{-1}) and TIBA were purchased from Amersham Biosciences (Buckinghamshire, UK) and Aldrich Chemical Company Inc. (USA), respectively. IBA, IAA, NAA, 2,4-D, 1,4-bis (5-phenyl-2-oxazolyl) benzene and 2,5-diphenyloxazole were purchased from Sigma. All other reagents and solvents (analytical grade) were obtained from Guangzhou Chemical Reagent Company (Guangzhou, China). IAA and TIBA solutions were filter-sterilized and the other auxins solutions were sterilized at 121°C for 15 min.

Pre-treatment of embryos with auxins and TIBA

To investigate the influence of IAA, IBA, NAA, 2,4-D and TIBA on root formation, selected embryos were pre-treated with indicated concentrations of growth regulators (see Tables 2–4) for 1 h, then crossly cut into 2-cm segments and cultured on AM as described above. To minimize a gravitropic response and IAA breakdown, pre-treatments were achieved on a shaker (60 rpm) at 28 ± 2°C in the dark.

PAT assay

Auxin transport in cotyledon segments, i.e., the movement of auxin in acropetal direction (from PCS to DCS) or basipetal direction (from DCS to PCS) was measured according to a published procedure (Martin et al. 2003). Cotyledon segments (2 cm in length) were labeled with [^{3}H]IAA before rooting. To study the direction of auxin movement (i.e., from PCS to DCS or vice versa), segments were placed on sterilized filter paper (with PCS or DCS as upper surface). After segment excision, four 5-µl tepid AM drops containing [^{3}H]IAA were applied to the cut surface. This treatment was performed within 10 min after excision, in order to preclude the loss of polar transport capacity of the cotyledon segments (Morris and Johnson 1990). The labeled AM drops contained 1 µM [^{3}H]IAA (four 5-µl AM drops ≈ 6,000 Bq) and 10 µM non-labeled IAA. Cold IAA was added because IAA concentrations higher than 1 µM resulted in increased auxin transport (Reed et al. 1998). The labeled segments were then incubated for the indicated time on solidified AM (0.7% agar, pH 5.8) at 28 ± 2°C in the dark. Segments were horizontally placed on AM (the unlabeled abaxial surfaces of cotyledon segments had direct contact with the AM). A 2 mm-end at the non-labeled site of each segment (either PCS or DCS) was excised and placed into a plastic scintillation vial (with screw lid) containing 2 ml of 100% methanol. After extraction of [^{3}H]IAA at 24 ± 2°C for 24 h, 10 ml of scintillation cocktail (6 g 2,5-diphenyloxazole and 0.5 g 1,4-bis (5-phenyl-2-oxazolyl) benzene in 667 ml toluene and 333 ml 2-ethoxyethanol) were added to each vial. After vortexing, samples were left overnight at 24 ± 2°C in the dark. Radioactivity was measured with a scintillation counter (liquid scintillation analyzer, model 2900 Tri-Carb; Packard Instruments Co., USA).

To study the effects of TIBA, NAA and IBA on PAT, embryos were treated with 100 µM TIBA, 2,700 µM NAA, 2,500 µM IBA or water (control) for 1 h. Embryos were then rinsed with distilled water, crossly cut into 2-cm segments, and labeled with a [^{3}H]IAA pulse as described above.

Histological observations

Cotyledon explants (pre-treated with 2,700 µM NAA or water controls) were cultured on AM for 0–14 days.

Table 2 Effects of auxins on adventitious root formation of cotyledon segments

Treatment	Percentage of rooting (%)	Rooting time (days)	Number of adventitious roots on the PCS	Number of adventitious roots on abaxial surfaces
Control (H_2O)	66.7 ± 8.8c	13.8 ± 0.4ab	7.3 ± 0.6c	0
57.1 μM IAA	62.8 ± 3.9c	14.8 ± 0.7a	5.2 ± 0.7cd	0
570.8 μM IAA	75.0 ± 2.9bc	13.5 ± 0.8ab	6.5 ± 0.8cd	0
2,900 μM IAA	86.7 ± 3.3ab	13.1 ± 0.5abc	13.0 ± 1.3b	0
49.2 μM IBA	63.3 ± 8.8c	13.4 ± 0.6ab	4.7 ± 0.7cd	0
492.1 μM IBA	85.6 ± 2.9ab	11.2 ± 0.4d	11.5 ± 0.9b	0
2,500 μM IBA	90.0 ± 5.7ab	11.0 ± 0.3d	17.7 ± 1.2a	0
53.7 μM NAA	58.9 ± 4.8c	12.9 ± 0.6bc	4.2 ± 0.5d	0
537.4 μM NAA	73.3 ± 6.7bc	11.7 ± 0.8cd	6.7 ± 0.7cd	0
2,700 μM NAA[a]	94.7 ± 2.7a	9.3 ± 0.2e	7.0 ± 0.6cd	30.2 ± 1.5
45.2 μM 2,4-D	0	–	0	0
226.2 μM 2,4-D	0	–	0	0
452.4 μM 2,4-D	0	–	0	0

Embryos were pre-treated with the indicated concentrations of auxins or water (control). Embryos were then crossly cut into 2-cm segments. The cotyledon segments were cultured on AM for 28 days. Values represent means ± SE from three independent experiments with at least 30 segments per treatment. Values within a column followed by the same letter are not significantly ($P > 0.05$) different according to Duncan's multiple range test

[a] For cotyledon segments pre-treated with 2,700 μM NAA, the percentage of rooting and the rooting time were determined for adventitious roots that emerged on abaxial surfaces

Table 3 Effects of TIBA on adventitious root formation on the PCS of cotyledon segments

Treatment	Percentage of rooting (%)	Rooting time (days)	Number of adventitious roots on the PCS
Control (H_2O)	66.7 ± 8.8a	13.8 ± 0.4b	7.3 ± 0.6a
20 μM TIBA	40.0 ± 5.8b	15.9 ± 0.6ab	4.4 ± 0.7b
100 μM TIBA	16.7 ± 3.3c	17.4 ± 1.1a	2.2 ± 0.4c
200 μM TIBA	0	–	0

Embryos were pre-treated with indicated concentrations of TIBA or water (control) and then cut into 2-cm segments. The cotyledon segments were cultured on AM for 28 days. Values represent means ± SE from three independent experiments with at least 20 segments per treatment. Values within the column followed by the same letter are not significantly ($P > 0.05$) different according to Duncan's multiple range test

At the time of harvest, plant material was fixed in FAA (formalin:acetic acid:ethanol = 5:5:90 v/v/v) for 24 h. Samples were then stained with Schiff's reagent, dehydrated with increasing concentrations of alcohol and embedded in paraffin. Seven-μm thick sections were cut with a microtome. After de-waxing in xylene, sections were stained with 0.5% toluidine blue. Observations were made with a light microscope.

Statistical analysis

Data were analyzed using analysis of variance (ANOVA) followed by Duncan's multiple range test at a 5% level.

Results

Two distinct patterns of adventitious root formation

Depending on different pre-treatments, two patterns of adventitious roots could be induced from cotyledon segments of mature mango embryos (Fig. 1). A first pattern of root formation was observed on the PCS near the embryo axis, whereas no roots were formed on the opposite site, the DCS (Fig. 1f–h). When embryos were pre-treated with 2,700 μM NAA for 1 h, a second pattern of root formation was seen on abaxial surfaces of cotyledon segments (Fig. 1j–l).

Table 4 Effects of TIBA and NAA on adventitious root formation of cotyledon segments

Treatment with NAA + TIBA (μM)	Percentage of rooting[a] (%)	Rooting time[a] (days)	Number of adventitious roots on the PCS	Number of adventitious roots on the abaxial surface
2,700 + 0	94.7 ± 2.7a	9.3 ± 0.2b	7.0 ± 0.6a	32.3 ± 1.8a
2,700 + 100	83 ± 6.5ab	12.9 ± 0.7a	2.3 ± 0.5b	8.9 ± 1.7b
2,700 + 200	68.1 ± 3.7b	13.8 ± 0.9a	0	7.1 ± 1.1b

Embryos were pre-treated with the indicated concentrations of NAA and TIBA and then cut into 2 cm segments. The cotyledon segments were cultured on AM for 28 days. Values represent means ± SE from three independent experiments with at least 20 segments per treatment. Values within the column followed by the same letter are not significantly ($P > 0.05$) different according to Duncan's multiple range test

[a] The percentage of rooting and the rooting time were determined for adventitious roots that emerged on the abaxial surface

Adventitious roots on the PCS and the effect of plant growth regulators

After removal of the embryo axis, mango cotyledons were crossly (Fig. 1b) or longitudinally (Fig. 1c) cut into 2-cm long segments, resulting in PCS, DCS, LCS, abaxial and adaxial surfaces (Fig. 1b–d). Segments cultured on AM for 14 days showed first adventitious roots on the PCS and more roots emerged during the following days (Fig. 1f). These adventitious roots were only formed on the PCS, whereas no roots emerged from the DCS or the LCS (Fig. 1f–i). Segments cultured for 28 days exhibited about seven roots. All adventitious roots emerged in the peripheral zone of the PCS, which contained vascular bundles (VB) (Fig. 1e).

The length of cotyledon segments significantly affected the formation of adventitious roots on the PCS (Table 1). When the segment length was shortened from 2 cm to 5 mm, the percentage of rooting and the number of adventitious roots on the PCS was significantly lower. No adventitious roots emerged from short segments (2 mm in length), even when incubated for 28 days. The rooting time also depended on the segment length. In 5-mm segments for example, the rooting was about 2 days delayed compared to 2-cm segments.

We further studied the effect of IAA or IBA on adventitious root formation. Embryos were pre-treated with different concentrations of IAA or IBA and then cut into 2-cm long cotyledon segments, which were cultured on AM in the dark for the indicated time. As shown in Table 2, pre-treatments with IAA or IBA showed dose-dependent effects: (i) low concentrations of IAA (57.1 μM) and IBA (49.2 μM) exhibited little effects on the percentage of rooting. When concentrations of IAA and IBA were elevated 10-fold, IBA (492.1 μM) significantly increased the percentage of rooting. High pre-treatment concentrations of either IAA (2,900 μM) or IBA (2,500 μM) significantly promoted the percentage of rooting. (ii) Low concentrations of IAA (57.1 and 570.8 μM) or IBA (49.2 μM) had little effects on the number of adventitious roots emerged on the PCS. Pre-treatments with higher concentrations of IAA (2,900 μM) or IBA (492.1 μM) significantly increased the number of roots and 2,500 μM of IBA induced most pronounced effects. (iii) High concentrations of IBA (492.1 or 2,500 μM) significantly shortened the rooting time. On the other hand, pre-treatments with all tested concentrations of IAA barely affected the rooting time (Table 2).

In contrast to IAA and IBA, pre-treatments with 2,4-D blocked adventitious root formation (Table 2), and only some tumor-like structures were induced on abaxial surfaces of cotyledon segments.

We further tested the effect of the auxin transport inhibitor TIBA on adventitious root formation. Pre-treatments with 20 and 100 μM TIBA significantly reduced the percentage of rooting and also decreased the number of roots that emerged on the PCS. Furthermore, a pre-treatment with 200 μM TIBA completely inhibited adventitious root formation (Table 3).

Pre-treatment with NAA results in adventitious root formation on abaxial surfaces of cotyledon segments

Unlike with IBA and IAA, a pre-treatment of embryos with high concentrations of NAA (2,700 μM) induced adventitious root formation on

abaxial surfaces of cotyledon segments (Fig. 1k, l and Table 2), indicating another pattern of adventitious root formation. The adventitious roots emerged from several narrow 'canal' regions, where vascular strands are located (Fig. 1k, l). The pre-treatment with 2,700 μM NAA strongly increased the percentage of rooting and the number of adventitious roots on abaxial surfaces. Moreover, the rooting time was shortened (Table 2).

It is worth noting that the pre-treatment with 2,700 μM NAA did not significantly change the number of roots emerged from the PCS of a given cotyledon segment (Table 2). In contrast, when embryos were pre-treated with low concentrations of NAA (53.7 μM), the number of adventitious roots on the PCS significantly decreased. A pre-treatment with 537.4 μM of NAA slightly shortened the rooting time for roots that emerged on the PCS, but had little effects on the percentage of rooting and the number of roots on the PCS (Table 2).

Pre-treatments with a combination of NAA (2,700 μM) and TIBA inhibited root formation on both, the PCS and abaxial surfaces of cotyledon segments (Table 4). An application with 2,700 μM NAA and 100 μM TIBA reduced the percentage of rooting from 94.7 to 83% and significantly inhibited the number of adventitious roots. A pre-treatment with 2,700 μM NAA and 200 μM TIBA completely blocked the formation of roots on the PCS, whereas few roots still emerged on the abaxial surface (Table 4).

Histological observations

Histological observations showed that there were about 6–9 vascular strands below the abaxial surface of a cotyledon half, which all almost extended in a parallel direction (Fig. 2a, b). Each vascular bundle had a well-developed laticiferous canal in the phloem. The canal cavity (CC in Fig. 2c) was surrounded by several cell layers. The innermost cell layer appeared to be secretory (epithelial cells) and was surrounded by a sheath of thin-walled, elongated parenchymal cells (EP in Fig. 2c). Prior emergence of roots from PCS, first divisions of parenchymal cells of phloem adjacent to the sheath were observed in cotyledon segments cultivated for about 6 days. These meristematic cells had a small size and a darkly stained cytoplasm (Fig. 2d, e). Continuation of cell divisions resulted in the formation of an annular structure (AS in Fig. 2f). Thereafter, the cells only divided tangentially toward the PCS. Adventitious root primordia (RP in Fig. 2g, h) were formed in cotyledon segments cultivated for about 10 days and first roots emerged from the PCS about 4 days later (Fig. 2i, j).

Similar to adventitious root formation on PCS, roots on abaxial surfaces (induced by the pre-treatment with 2,700 μM NAA) also originated from a sheath of parenchymal cells of phloem. Whereas roots on the PCS were formed close to vascular bundles (in the peripheral zone of the PCS), the NAA-induced roots emerged on abaxial surfaces, i.e., in vertical direction to the vascular strands (Fig. 3i, j). Cell divisions of phloem parenchymal cells resulted in formation of an annular structure. The direction of the cell was strictly acropetal, i.e., toward the abaxial surface (on the opposite site of the xylem) (Fig. 3d). Thereafter, a root primordium was developed from these newly formed meristem-like cells (Fig. 3f) and the roots emerged on the abaxial surface of the cotyledon segment (Fig. 3i, j and Fig. 1k, l).

Relationship between PAT and adventitious root formation

To determine the role of PAT during adventitious root formation, [^{3}H]IAA was used to assess the auxin transport in cotyledon segments. We defined the auxin transport from DCS to PCS as basipetal auxin transport, and the transport from PCS to DCS as acropetal auxin transport. As shown in Table 5, basipetal transport of [^{3}H]IAA was measured as early as 4 h after labeling. The amount of [^{3}H]IAA was further increased during the following hours (Table 5), and remained then at an approximately constant level (data not shown). In contrast, acropetal transport of [^{3}H]IAA was low and did not change during the experiment (Table 5). These data indicate that cotyledon segments transported IAA in the basipetal direction (i.e., from DCS to PCS).

As shown in Fig. 4, a pre-treatment with 100 μM TIBA significantly ($P < 0.001$) reduced the basipetal transport of [^{3}H]IAA (decrease from 58.8 Bq g^{-1} FW to 9.4 Bq g^{-1} FW). The pre-treatment had little effects on the acropetal transport of [^{3}H]IAA, however. Interestingly, pre-treatments with 2,500 μM IBA or 2,700 μM NAA, which showed strong effects on

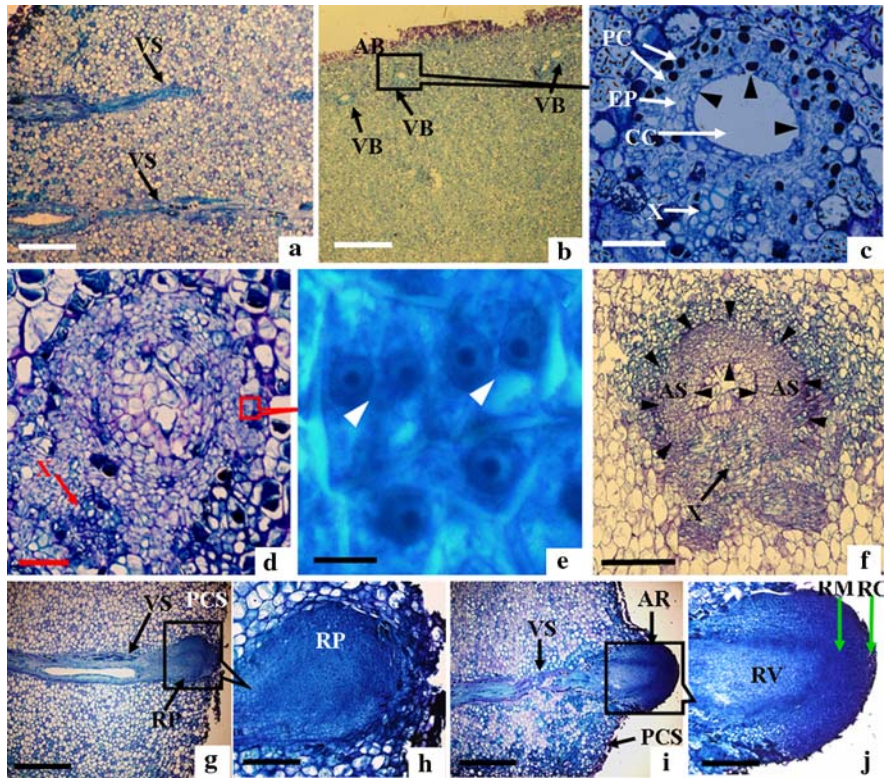

Fig. 2 Histological observation of adventitious root formation on the PCS of cotyledon segments. Mature embryos were cut into 2-cm cotyledon segments, which were either microscopically analyzed (day 0) or incubated on AM in the dark for the indicated number of days. At the time of harvest, 2-mm thin tissue slices near the PCS were fixed in FAA for 24 h. Slices at right angles to the long axis of the cotyledon (or root) are defined as cross sections. Slices in parallel to the long axis of the cotyledon (or root) are defined as longitudinal sections. Cross (**b**–**f**) and longitudinal (**a**, **g**–**j**) sections were stained with Schiff's reagent and 0.5% toluidine blue. (**a**) Longitudinal section of a cotyledon segment (day 0) with vascular strands (VS). Bar = 500 μm. (**b**) Cross section of a cotyledon segment (day 0) with vascular bundles (VB) below the abaxial surface (AB). Bar = 500 μm. (**c**) Details of boxed area of (**b**). Each vascular bundle had a well-developed laticiferous canal located in the phloem; the canal cavity (CC) was surrounded by several cell layers, the innermost cell layer appears to be secretory (*arrowheads*). This layer is surrounded by a sheath of thin-walled, elongated parenchymal cells (EP). Bar = 100 μm. (**d**) Parenchymal cells of phloem (PC) adjacent to the sheath of EP (day 6). Bar = 100 μm. (**e**) Details of boxed area in (**d**), showing induced meristem-like cells; these cells were small in size and had a darkly stained cytoplasm; some cells are in the stage of cell division (*arrowheads*). Bar = 10 μm. (**f**) Parenchymal cells continued to divide and formed (radial symmetric to the CC) an annular structure (AS, *arrowheads*; day 10). Bar = 100 μm. (**g**) Finally, an adventitious root primordium (RP) connected to VS was formed at the PCS (day 10). Bar = 200 μm. (**h**) Details of boxed area in (**g**), showing the structure of the RP. Bar = 700 μm. (**i**) Emergence of an adventitious root (AR) connected to VS at the PCS (day 14). Bar = 800 μm. (**j**) Details of boxed area in (**i**), showing the structure of the AR. Bar = 300 μm. Abbreviations: AB, abaxial surface; AR, adventitious root; AS, annular structure; EP, elongated parenchymal cells; PC, parenchymal cells of phloem; PCS, proximal cut surface; RC, root cap; RM, root meristem; RP, adventitious root primordium; RV, root vascular cylinder; VB, vascular bundles; VS, vascular strands; X, xylem

adventitious root formation (Table 2), did not significantly affect the basipetal transport of [^{3}H]IAA (Fig. 4).

Discussion

In this study, we report two patterns of adventitious root formation in cotyledon segments of mango plants. Our findings differ from rooting patterns in cotyledon segments from other plants, where adventitious roots emerged either on tips of elongating petioles or at the proximal end of cotyledon fragments (Ermel et al. 2000; Gonzalez et al. 1991; Jay-Allemand et al. 1991). In our mango cotyledon segments, a first pattern of adventitious roots was

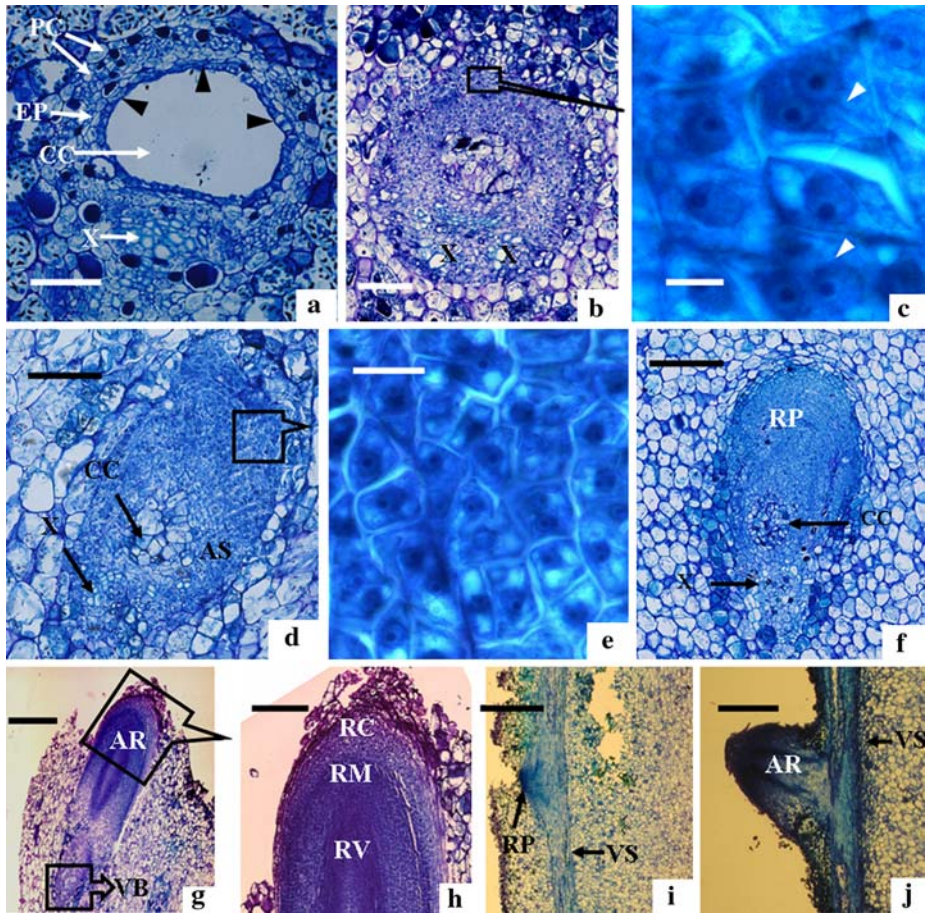

Fig. 3 Histological observations of NAA-induced adventitious roots on the abaxial surface of cotyledon segments. Mature embryos were pre-treated with 2,700 μM NAA and then cut into 2-cm cotyledon segments, which were either directly microscopically analyzed (day 0) or incubated on AM in the dark for the indicated number of days. At the time of harvest, explants were fixed in FAA for 24 h. Cross (**a**–**h**) and longitudinal (**i**–**j**) sections were stained with Schiff's reagent and 0.5% toluidine blue. (**a**) Cross section of a cotyledon segment (day 0). Each vascular bundle has a well-developed laticiferous canal located in the phloem; the canal cavity (CC) was surrounded by several cell layers, the innermost layer of cells appeared to be secretory (*arrowheads*) and was surrounded by a sheath of thin-walled, elongated parenchymal cells (EP). Bar = 100 μm. (**b**) The parenchymal cells of phloem (PC in (**a**)) adjacent to the sheath of EP (day 4). Bar = 100 μm. (**c**) Details of boxed area of (**b**), showing the induced meristem-like cells; these cells were small in size and had a darkly stained cytoplasm; some cells are in the stage of cell division (*arrowheads*). Bar = 10 μm. (**d**) Parenchymal cells repeatedly divided and formed (radial symmetric to the CC) an annular structure (AS); Thereafter, only a part of newly formed cells of the AS divided further. These dividing cells (above the CC) were on the site of the abaxial surface and faced the xylem (X) of the cotyledon. The cells subsequently divided in the acropetal direction (towards the abaxial surface of the cotyledon segment) and a new cell layer was formed above of the CC (day 6) (**e**) Details of boxed area of (**d**), showing the induced meristem-like cells; these cells were small in size and had a darkly stained cytoplasm. Bar = 30 μm. (**f**) Continuation of cell divisions in the acropetal direction resulted in formation of an adventitious root primordium (RP) on the opposite site of the xylem (day 7). Bar = 200 μm. (**g**) Emergence of an adventitious root (AR) on the abaxial surface of the cotyledon segment (day 10); the root is connected with a vascular bundle (VB). Bar = 50 μm. (**h**) Details of boxed area of (**g**), showing the root structure. Bar = 150 μm. (**i**) The RP (day 7) is connected with a vascular strand (VS). Bar = 800 μm. (**j**) An adventitious root broken through the abaxial surface of the cotyledon segment (day 10). The root was formed in vertical direction to the vascular strand. Bar = 800 μm. Abbreviations: AR, adventitious root; AS, annular structure; EP, elongated parenchymal cells; PC, parenchymal cells of phloem; RC, root cap; RM, root meristem; RP, adventitious root primordium; RV, root vascular cylinder; VB, vascular bundles; VS, vascular strands; X, xylem

Table 5 [^{3}H]IAA transport in cotyledon segments

Transport period (h)	Basipetal transport (Bq g^{-1} FW)	Acropetal transport (Bq g^{-1} FW)
3	2.3 ± 0.5c	2.2 ± 0.4a
4	15.7 ± 2.9b	2.3 ± 0.3a
6	60.5 ± 8.0a	2.5 ± 1.0a
8	66.8 ± 11.1a	3.3 ± 0.4a

Cotyledon segments were excised from mature embryos. Segments were then placed on a sterilized filter paper and labeled with [^{3}H]IAA as described in "Materials and methods." After the indicated time of incubation (transport period), a 2-mm slice at the non-labeled end was excised and used for measurement of radioactivity. Values correspond to means ± SE from at least 10 segments. Values within a column followed by the same letter are not significantly ($P > 0.05$) different according to Duncan's multiple range test

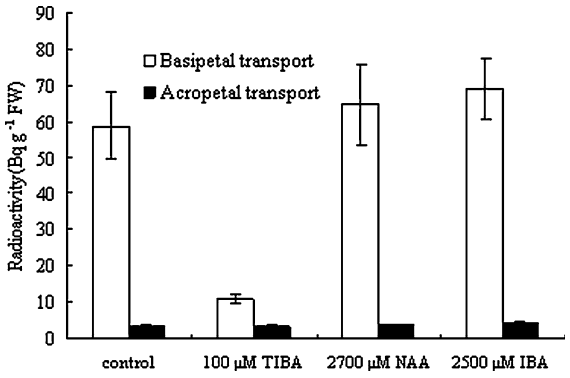

Fig. 4 [^{3}H]IAA transport in cotyledon segments pre-treated with different plant growth regulators. Embryos were pre-treated with water (control), 100 μM TIBA, 2,700 μM NAA or 2,500 μM IBA for 1 h. [^{3}H]IAA was applied to excised 2-cm cotyledon segments as described in "Materials and methods." Radioactivity at the non-labeled end was measured after incubation of 8 h. Values represent means ± SE from at least 10 segments

observed at the PCS in the region of vascular bundles (Fig. 1e–i). When pre-treated with 2,700 μM NAA, a second pattern of adventitious root was seen on abaxial surfaces of cotyledon segments. Emergence of these roots was restricted to several narrow 'canal' regions in the region of the cotyledon's vascular strands (Fig. 1k, l). Interestingly, pre-treatments with IAA, IBA or low concentrations of NAA did not induce adventitious root formation on abaxial surfaces (Table 2). All tested plant growth regulators used in this study were unable to stimulate adventitious root formation on the DCS. These findings, together with our histological observations (Figs. 2, 3), suggest that adventitious root formation in cotyledon segments is controlled by positional effects, which are related to vascular strands.

Histological origin of adventitious roots

In flowers, fruits, young stems and leaves of mango plants, laticiferous canals originate from parenchymal cells of phloem. These canals are formed schizo-lysigenously or lysigenously, resulting in vascular bundles containing a laticiferous canal (Venning 1948). Similarly, in cotyledon segments of mango, each vascular bundle possesses a well-developed laticiferous canal in the phloem (Fig. 2b, c). Our histological observations showed that adventitious root formation on the PCS or on abaxial surfaces originated from parenchymal cells of phloem adjacent to a sheath, which surrounded the canal cavity. This observation is reminiscent to adventitious root formation in hypocotyl and epicotyl cuttings of *Pinus strobus* (Goldfarb et al. 1998) and *Pinus radiata* (Smith and Thorpe 1975), two species that also form laticiferous canals. In contrast, adventitious roots from cotyledon explants of *Juglans regia* originated from perifascicular cells in elongating petioles (Ermel et al. 2000).

Our work shows two distinct patterns of adventitious roots that were differently initiated. Root development on the PCS was preceded by formation of an annular structure (Fig. 2f). As cells only divided tangentially (toward the PCS), a root primordium was formed within these newly formed cells. Consequently, adventitious roots emerged on the PCS (Fig. 2g–j). In contrast, root formation on abaxial surfaces induced by NAA was different. After formation of an annular structure, only specific cells (close to the abaxial surface and facing the xylem) continued to divide. Cells divided in the acropetal direction, resulting in an adventitious root primordium that was located exterior to the xylem (Fig. 3d–h).

PAT appears to be associated with adventitious root formation on the PCS of cotyledon segments

Our results suggest that PAT might play a key role in adventitious root formation on the PCS. Embryos pre-treated with high concentrations of IAA or IBA for 1 h exhibited increased root formation (Table 2)

and TIBA, a well-known inhibitor of PAT (Depta et al. 1983; Martin et al. 1987; Yang et al. 2006) inhibited root formation in a dose-dependent manner (Table 3). On the other hand, pre-treatments with low concentrations of IAA or IBA did not affect the percentage of rooting and the number of adventitious roots (Table 2). These findings are in agreement with the results of Díaz-Sala et al. (1996) who reported that only a continuous IBA pre-treatment promoted rooting in loblolly pine hypocotyls, whereas a short IBA pulse had no effects.

Our microscopical investigations also point towards a role of PAT in adventitious root formation. Cotyledon sections showed that adventitious roots on PCS were initiated from vascular tissue. Indeed, vascular strands are well known to play an important function in transport of auxin and other plant growth regulators (Moore 1989; Rubery 1987).

The experiments with [^{3}H]IAA in this study show that auxin in cotyledon segments was transported in the basipetal direction (Table 5). As auxin flow was significantly inhibited by pre-treatment with TIBA (Fig. 4), it is likely that TIBA blocked auxin transport and consequently adventitious root formation on the PCS (Table 3). However, it has been reported that TIBA has the potential to act as anti-auxin and thus may inhibit auxin action (Depta and Rubery 1984). Therefore, inhibitory effects of TIBA on adventitious root formation could be, at least in part, a consequence of inhibited auxin action. Future experiments with auxin transport inhibitors other than TIBA are required to distinguish between effects on auxin transport and auxin action.

It is worth noting that the pre-treatments with 2,500 μM IBA or 2,700 μM NAA did not significantly alter PAT (Fig. 4), although the former promoted adventitious root formation on the PCS and the latter induced adventitious roots on abaxial surfaces. The effects of IBA in our study are consistent with the findings of Fords et al. (2002), which showed no obvious change of PAT in IBA-treated *Forsythia* plants, although the rooting ability was stimulated by IBA. In addition, pre-treatments with 2,4-D blocked adventitious root formation (Table 2). This finding is in agreement with the results of Gao et al. (2005) and Metivier et al. (2007), who reported that 2,4-D treatments did not lead to adventitious root formation in the explants of *Panax notoginseng* and *Cotinus coggygria*.

Rooting responses in our study were dramatically affected by the length of the segment. A minimal length of 5 mm was required for rooting (Table 1). A similar phenomenon was reported by Marks et al. (2002) for *Forsythia* and *Syringa* internodes, where rooting depended on the internode size. We suggest that rhizogenesis factors are transported from the end of the cotyledon to the embryo axis. One possibility is that the levels of these rhizogenesis factors are higher in longer cotyledon segments and that sufficient amounts of rhizogenesis factors on the PCS are required for initiation of cell division. Our data suggest that the amounts of rhizogenesis factors in cotyledon segments shorter than 2 mm are not sufficient for induction of adventitious roots. The rhizogenesis factors include most likely auxin, and perhaps also flavonoids. It has been reported that flavonoids are released during wounding and that they have the ability to act as negative regulators of auxin transport (Jacobs and Rubery 1988).

NAA initiates adventitious root formation on abaxial surfaces of cotyledon segments

We show in this work that adventitious root formation on abaxial surfaces of cotyledon segments was induced by a pre-treatment with 2,700 μM NAA. Various publications reported that the dedifferentiation phase can be triggered or promoted by anti-auxins and stress treatments as well as auxins (Shibaoka 1971; Kikuchi et al. 2006). NAA may act either as a stress substance or as an auxin that triggers dedifferentiation of cells that form the root primordium. Interestingly, when we simultaneously pre-treated embryos with a combination of 2,700 μM NAA and TIBA (an inhibitor of auxin efflux carriers), rooting of cotyledon segments was significantly reduced (Table 4). This finding provides additional evidence that PAT also plays a role in adventitious root formation on abaxial surfaces. We suggest that NAA may function as an auxin rather than a stress substance.

It has been shown that NAA enters cells mainly by diffusion, i.e. not carrier mediated. NAA is a good substrate for auxin efflux carriers, however. In contrast, IAA influx and efflux carriers exhibit a high affinity for IAA. Transport of IAA is therefore controlled by both carriers (Delbarre et al. 1996;

Morris et al. 2004; Yamamoto and Yamamoto 1998). Thus, when supplied at similar concentrations, NAA influx by diffusion is more efficient than IAA (or IBA), resulting in higher levels of NAA in target cells. In tobacco explants for example, NAA was taken up six times faster than IAA (Peeters et al. 1991; Smulders et al. 1988). This may explain our findings that high concentrations of NAA (2,700 μM) stimulated adventitious root formation on abaxial surfaces of cotyledon segments. We suggest that a minimal threshold level of NAA is required to trigger root primordium initiation, and this threshold level will be reached by the balance between the diffusion influx and carrier mediated efflux of NAA. Similar differences between NAA and IBA treatments have been reported for the rooting ability of hypocotyl and epicotyl explants in *Pinus strobus* (Goldfarb et al. 1998).

Taken together, we describe in this paper two patterns of adventitious root formation in cotyledon segments of mango plants. The data from our experiments with auxins, TIBA and [^{3}H]IAA point to an important role of PAT in adventitious root formation. Future experiments are required to understand the molecular mechanisms underlying flow and action of auxin during root organogenesis in tree species.

Acknowledgements This work was supported by a grant from the National Natural Science Foundation of China (30470110).

References

Blakesley D (1994) Auxin metabolism and adventitious root initiation. In: Davis TD, Haissig BE (eds) Biology of adventitious root formation. Plenum Press, New York, pp 143–154

De Klerk GJ, Van der Krieken W, De Jong JC (1999) The formation of adventitious roots: new concepts, new possibilities. In Vitro Cell Dev Biol-Plant 35:189–199

Delbarre A, Muller P, Imhoff V, Guern J (1996) Comparison of mechanisms controlling uptake and accumulation of 2,4-dichlorophenoxyacetic acid, naphthalene-1-acetic acid and indole-3-acetic acid in suspension-cultured tobacco cells. Planta 198:532–541

Depta H, Eisle KH, Hertel R (1983) Specific inhibitors of auxin transport: action on tissue segments and in vitro binding to membranes from maize coleoptiles. Plant Sci Lett 31:181–192

Depta H, Rubery PH (1984) A comparative study of carrier participation in the transport of 2,3,5-triiodobenzoic acid, indole-3-acetic acid, and 2,4-dichlorophenoxyacetic acid by *Cucurbita pepo* L. hypocotyl segments. J Plant Physiol 115:371–387

Díaz-Sala C, Hutchison KW, Goldfarb B, Greenwood MS (1996) Maturation-related loss in rooting competence by loblolly pine stem cuttings: the role of auxin transport, metabolism and tissue sensitivity. Physiol Plant 97: 481–490

Ermel FF, Vizoso S, Charpentier JP, Jay-Allemand C, Catesson AM, Couée I (2000) Mechanisms of primordium formation during adventitious root development from walnut cotyledon explants. Planta 211:563–574

Ford YY, Bonham EC, Cameron RWF, Blake PS, Judd HL, Harrison-Murra RS (2002) Adventitious rooting: examining the role of auxin in an easy- and a difficult-to-root plant. Plant Growth Regul 36:149–159

Gao XF, Zhu CB, Jia W, Gao WY, Qiu MF, Zhang YY, Xiao PG (2005) Induction and characterization of adventitious roots directly from the explants of *Panax notoginseng*. Biotechnol Lett 27:1771–1775

Goldfarb B, Hackett WP, Furnier GR, Mohn CA, Plietzsch A (1998) Adventitious root initiation in hypocotyl and epicotyl cuttings of eastern white pine (*Pinus strobus*) seedlings. Physiol Plant 102:513–522

Gonzalez A, Rodriguez R, Tames RS (1991) Ethylene and in vitro rooting of hazelnut (*Corylus avellana*) cotyledons. Physiol Plant 81:227–233

Gutmann M, Charpentier JP, Doumas P, Jay-Allemand C (1996) Histological investigation of walnut cotyledon fragments for a better understanding of in vitro adventitious root initiation. Plant Cell Rep 15:345–349

Jacobs M, Rubery PH (1988) Naturally occurring auxin transport regulators. Science 241:346–349

Jarvis BV, Shaheed AF (1986) Adventitious root formation in relation to the uptake and distribution of supplied auxin. New Phytol 103:23–31

Jay-Allemand C, De Pons V, Doumas P, Capelli P, Sossountzov L, Cornu D (1991) Formation de racines in-vitro à partir de cotylédon de noix (*Juglans* sp.): un modèle de la rhizogenèse chez les espèces ligneuses. CR Acad Sci Paris 312:369–375

Kevers C, Hausman JF, Faivre-Rampant O, Evers D, Gaspar T (1997) Hormonal control of adventitious rooting: progress and questions. Angew Bot 71:71–79

Kikuchi A, Sanuki N, Higashi K, Koshiba T, Kamada H (2006) Abscisic acid and stress treatment are essential for the acquisition of embryogenic competence by carrot somatic cells. Planta 223:637–645

Liu JH, Reid DM (1992) Adventitious rooting in hypocotyls of sunflower (*Helianthus annuus*) seedlings. IV. The role of changes in endogenous free and conjugated indole-3-acetic acid. Physiol Plant 86:285–292

Ljung K, Östin A, Lioussanne L, Sandberg G (2001) Developmental regulation of indole-3-acetic acid turnover in Scots pine seedlings. Plant Physiol 125:464–475

López Nicolás JL, Acosta M, Sánchez-Bravo J (2004) Role of basipetal auxin transport and lateral auxin movement in rooting and growth of etiolated lupin hypocotyls. Physiol Plant 121:294–304

Marks TR, Ford YY, Cameron RWF, Goodwin C, Myers. PE, Judd HL (2002) A role for polar auxin transport in rhizogenesis. Plant Cell Tiss Org Cult 70:189–198

Martin HV, Beffa R, Pilet PE (1987) A comparison between 3,5-diiodo-4-hydoxybenzoic acid and 2,3,5-triiodobenzoic acid. II. Effects on uptake and efflux of IAA in maize roots. Physiol Plant 71:37–43

Martin F, Lindsey AH, Allison EC, Nicholas RS, David EF, Elizabeth VV (2003) Light interacts with auxin during leaf elongation and leaf angle development in young corn seedlings. Planta 216:366–376

Mensuali-Sodi A, Panizza M, Tognoni F (1995) Endogenous ethylene requirement for adventitious root induction and growth in tomato cotyledons and lavandin microcuttings in-vitro. Plant Growth Regul 17:205–212

Metivier PSR, Yeung EC, Patel KR, Thorpe TA (2007) *In vitro* rooting of microshoots of *Cotinus coggygria* Mill, a woody ornamental plant. In Vitro Cell Dev Biol-Plant 43:119–123

Moore TC (1989) Biochemistry and physiology of plant hormones. Springer-Verlag, New York

Morris DA, Johnson CF (1990) The role of auxin efflux carriers in the reversible loss of polar auxin transport in the pea (*Pisum sativum* L.) stem. Planta 181:117–124

Morris DA, Friml J, Zažímalová E (2004) The transport of auxins. In: Davies PJ (ed) Plant hormones: biosynthesis, signal transduction, action! Kluwer Academic Publisher, Dordrecht, pp 437–470

Normanly J, Cohen JD, Fink GR (1993) *Arabidopsis thaliana* auxotroph reveal a tryptophan-independent biosynthetic pathway for indole-3-acetic acid. Proc Natl Acad Sci USA 90:10355–10359

Peeters AJM, Gerads W, Barendse GWM, Wullems GJ (1991) In vitro flower bud formation in tobacco: interaction of hormones. Plant Physiol 97:402–408

Reed RC, Brady SR, Muday GK (1998) Inhibition of auxin movement from the shoot into the root inhibits lateral root development in *Arabidopsis*. Plant Physiol 118:1369–1378

Rubery PH (1987) Auxin transport. In: Davies PJ (ed) Plant hormones and their role in plant growth and development. Kluwer Academic Publishers, Dordrecht, pp 341–362

Shibaoka H (1971) Effects of indoleacetic, p-chlorophenoxyisobutyric and 2,4,6-trichlorophenoxyacetic acids on three phases of rooting in Azukia cuttings. Plant Cell Physiol 12:193–200

Smith DR, Thorpe TA (1975) Root initiation in cuttings of *Pinus radiata* seedlings. I. Developmental sequence. J Exp Bot 26:184–192

Smulders MJM, Janssen GFE, Croes AF, Barendse GWM, Wullems GJ (1988) Auxin regulation of flower bud formation in tobacco explants. J Exp Bot 39:451–459

Steffens B, Wang J, Sauter M (2006) Interactions between ethylene, gibberellin and abscisic acid regulate emergence and growth rate of adventitious roots in deepwater rice. Planta 223:604–612

Venning FD (1948) The ontogeny of the laticiferous canals in the Anacardiaceae. Am J Bot 35:637–644

Yamamoto M, Yamamoto KT (1998) Differential effects of 1-naphthaleneacetic acid, indole-3-acetic acid and 2,4-dichlorophenoxyacetic acid on the gravitropic response of roots in an auxin-resistant mutant of Arabidopsis, *aux-1*. Plant Cell Physiol 39:660–664

Yang Y, Hammes UZ, Taylor CG, Schachtman DP, Nielsen E (2006) High-affinity auxin transport by the AUX1 influx carrier protein. Curr Biol 16:1123–1127